Eur. J. Mineral.
2003, **15**, 931-935

Spectroscopic 2D-tomography: Residual pressure and strain around mineral inclusions in diamonds

LUTZ NASDALA[1]*, FRANK E. BRENKER[2], JÜRGEN GLINNEMANN[3], WOLFGANG HOFMEISTER[1], TIBOR GASPARIK[4], JEFFREY W. HARRIS[5], THOMAS STACHEL[6] and INGO REESE[7]

[1]Institut für Geowissenschaften – Mineralogie, Johannes Gutenberg-Universität, D-55099 Mainz, Germany
[2]Institut für Mineralogie und Geochemie, Universität zu Köln, D-50674 Köln, Germany
[3]Institut für Mineralogie, Johann Wolfgang Goethe-Universität, D-60054 Frankfurt/Main, Germany
[4]Department of Geosciences, State University of New York at Stony Brook, Stony Brook, NY 11794, U.S.A.
[5]Division of Earth Sciences, University of Glasgow, Glasgow G12 8QQ, United Kingdom
[6]Department of Earth and Atmospheric Sciences, University of Alberta, Edmonton, Alberta T6G 2E3, Canada
[7]Jobin Yvon GmbH, Neuhofstr. 9, D-64625 Bensheim, Germany

Abstract: We have studied high-pressure inclusions (Ca-silicates, coesite, graphite) in three large diamonds, one from the Kankan district, Guinea, and the other two from the Panda kimberlite, Ekati diamond mines, Canada. Using the *in situ* point-by-point mapping technique with a confocal Raman system, the mineralogy of the inclusions, as well as their area distribution pattern (*e.g.*, of different Ca-silicate phases) and their order-disorder distribution pattern (shown for graphite/disordered carbon), were determined. Raman mapping of the host diamonds yielded 2D-tomographic pressure and strain distribution patterns and provided information on the residual pressure of the inclusions (~ 2.3 GPa for a coesite inclusion and ~ 2.6 GPa for a graphite inclusion). The inclusions are surrounded by haloes of significantly enhanced pressure, several hundred μm across. These haloes exhibit complex pressure relaxation patterns that consist of micro-areas affected by both compressive and dilative strain, with the latter being intensive enough to result in apparent "negative pressures".

Key-words: diamond, graphite, coesite, larnite, walstromite, Raman spectroscopy, high pressure inclusions

Introduction

Inclusions of high-pressure (HP) minerals in diamonds enable us to sample deep regions of the earth's mantle. The study of inclusions in diamond, therefore, provides unique information about the composition of the source region and the conditions of diamond formation. Studying inclusions using Raman spectroscopy adds to this knowledge by not only identifying the mineralogy and the structural state of the included HP phases, but also any deformation of the surrounding diamond lattice, which, in turn, may allow estimation of the P-T conditions in the source region (Rosenfeld & Chase, 1961). It is clear, however, that such analyses require the application of an *in situ* technique that can be applied below the surface in order to prevent the complete pressure relaxation of an HP inclusion due to its exposure to the sample surface during the preparation of polished microprobe mounts. The confocal Raman microprobe technique is very well suitable for such analysis. It has already been used to study HP inclusions in diamond, in particular, to determine the original pressures of the inclusions (*e.g.*, Sobolev *et al.*, 2000; Ye *et al.*, 2001; Gillet *et al.*, 2002), and to quantify the residual pressure and strain in the host diamond (*e.g.*, Izraeli *et al.*, 1999). The vibrational spectra provide barometric information, because lattice compression results in shortened bond lengths and, in consequence, increased frequencies of lattice vibrations. Calibrations of pressure-induced band shifts, for example, have been reported for diamond (Hanfland *et al.*, 1985; Boppart *et al.*, 1985) and for coesite (Hemley, 1987).

The present study reports preliminary results of a micro-Raman investigation of three diamonds with included HP phases. For the first time, the point-by-point mapping technique was used to visualise structural features at certain depth levels inside natural diamonds and produce two-dimensional (2D) tomographic images. Measurements were carried out (1) to determine the mineralogy and the internal structure of the inclusions, (2) to obtain information on the pressure under which the inclusions were trapped, and (3) to study strain and pressure relaxation patterns in the host diamond adjacent to the inclusions.

*Corresponding author: nasdala@uni-mainz.de

DOI: 10.1127/0935-1221/2003/0015-0931
0935-1221/03/0015-0931 $ 2.25

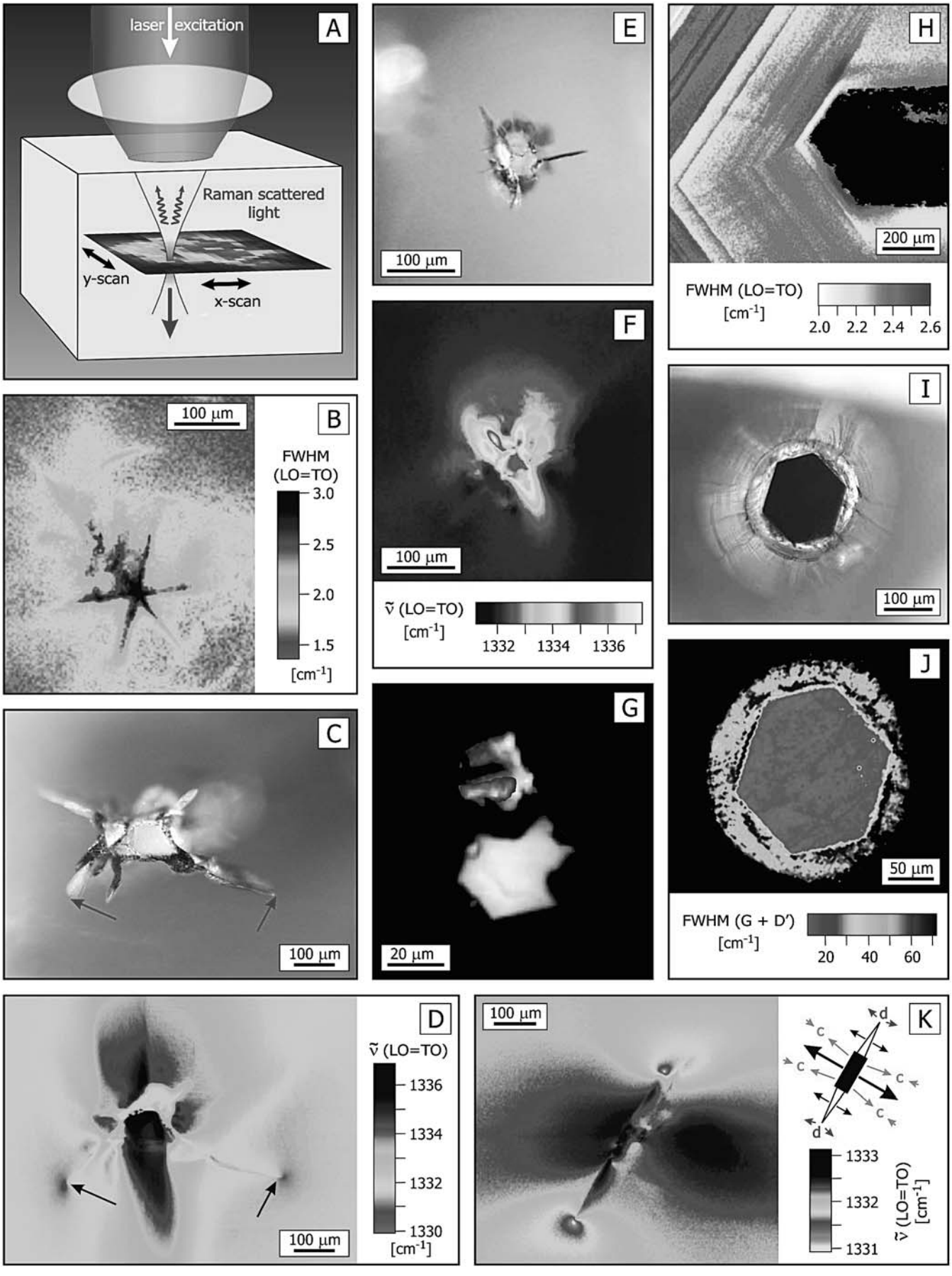
A
laser excitation
Raman scattered light
y-scan
x-scan
B
100 µm
FWHM (LO=TO)
3.0
2.5
2.0
1.5
[cm-1]
C
100 µm
D
100 µm
ν̃ (LO=TO)
1336
1334
1332
1330
[cm-1]
E
100 µm
F
100 µm
ν̃ (LO=TO) [cm-1]
1332 1334 1336
G
20 µm
H
200 µm
FWHM (LO=TO) [cm-1]
2.0 2.2 2.4 2.6
I
100 µm
J
50 µm
FWHM (G + D') [cm-1]
20 40 60
100 µm
K
d
c
c
c
c
d
1333
1332
1331
ν̃ (LO=TO) [cm-1]

Samples and experimental procedures

Diamond KK200 was recovered from the alluvial deposits in the Kankan district, Guinea. This crystal is about 10 mm in length and has a slightly distorted, somewhat rounded habit. It contains at least 20 mineral inclusions with sizes ranging from < 100 µm to ~ 1 mm. Inclusions are typically accompanied by radial fractures in the surrounding diamond (Fig. 1C, E). Diamonds PAG02 and PAG07 were collected from the production of the Panda kimberlite, part of the Ekati diamond mine, Northwest Territories, Canada. The octahedral crystals are ~ 2.5 mm in size, and each contains a graphite inclusion with plate-like habit. The graphite in PAG02 consists of numerous, uniformly oriented crystal flakes (Glinnemann *et al.*, 2003). Their (001) faces are oriented parallel to a (110) diamond face. The graphite in PAG07 is a large, idiomorphic crystal (Fig. 1I), with its (001) faces oriented parallel to a (111) diamond face. This graphite is surrounded by disk-shaped fractures in the same (111) diamond plane (Fig. 1I) whose formation is explained by extensive volume expansion of graphite along [001] upon pressure relaxation (Zhao & Spain, 1989).

On all three crystals, two faces were polished to serve as "windows". Although this is not necessary for an analysis, such preparation is advantageous for Raman mapping, since the removal of any surface roughness contributes to uniform experimental conditions.

Analyses were carried out using a Jobin Yvon LabRam HR system (focal length 80 cm) equipped with Olympus BX41 optical microscope and Si-based charge-coupled device detector. Spectra were excited with the He-Ne 632.816 nm line (3 mW at the sample). The wavenumber accuracy (calibrated using Ne lamp emissions) was 0.5 cm^{-1} and the spectral resolution was 0.8 cm^{-1}. Because laser light refraction at the air-diamond boundary and internal heterogeneity of the diamond affects the focus quality, sampling at depths of several hundred µm is tainted with impaired confocality. Depending on the actual sampling depth (which was 100-600 µm below the surface), the lateral resolution was of the order of several µm and the depth resolution was probably several tens of µm.

Raman mapping was done using an automatic, software-controlled x-y stage. For this, the sample is moved step-by-step relative to the fixed microscope objective (Fig. 1A). The step width was varied in the range 1-4 µm. A spectrum is obtained at each sampling point (*i.e.* for each pixel of the image to be generated). With the accumulation times of the order of one (diamond) to several seconds (inclusions) for each spectrum, it took 10 hours to 2 days to record mapping files containing 10,000-40,000 spectra. Since all spectral information is assigned to x-y-coordinates, colour-coded plots based on any spectral parameter can be generated after appropriate curve-fitting of the whole data set.

Results and discussion

High-pressure phases included in the three diamond samples were identified *in situ* using confocal Raman point analyses as a fingerprinting tool. The inclusions in PAG02 and PAG07 yielded the Raman pattern of graphite. Among 15 inclusions analysed in the diamond KK200, only one (#8) was found to be coesite. All the others are assemblages of Ca-silicates, which were identified as larnite (β-Ca_2SiO_4; see Reynard *et al.*, 1997), $CaSi_2O_5$ with titanite structure, and $CaSiO_3$ with walstromite structure. To confirm these assignments, we took reference spectra from an experimental product of Gasparik *et al.* (1994) that contained all three of the above Ca-silicates (Fig. 2). More detailed information on the inclusions was obtained using the Raman mapping technique. The order-disorder pattern of the graphite inclusion in PAG07 can be seen in a plot of the full width at half maximum (FWHM) of the main graphite band at ~ 1600 cm^{-1} (D' and G modes; Fig. 1J). Lateral distribution patterns of Ca-silicates within single inclusions in KK200 were accurately visualised in tomographic phase-contrast images (Fig. 1G).

Based on the results of Gasparik *et al.* (1994), the observation that all three Ca-silicate phases coexist in some inclusions (for example #9; Figs. 1E, G) points to rapid diamond uplift from conditions close to the Ca_2SiO_4 + $CaSi_2O_5 \leftrightarrow CaSiO_3$ phase boundary, *i.e.* ≥ 10 GPa (see Joswig *et al.*, 1999). The initial pressure must have been partially released through fracturing of the surrounding diamond upon heterogeneous expansion of the diamond-

Fig. 1 (opposite page). Raman maps of diamond samples and included HP phases. Spectral parameters that were used to generate maps are given individually in the subfigures. **(A)** Sketch of the experimental setup for 2D-tomographic maps. **(B)** Raman map of the diamond KK200 (view roughly along [11$\bar{1}$]) around inclusion #8 (coesite). The broadening of the diamond LO=TO mode reveals a strain pattern with a three-fold symmetry. **(C)** Microphotograph of the inclusion KK200-6 (Ca-silicates). **(D)** Raman map of diamond KK200 (same area as in C; view along [331]). Areas affected by dilative strain at the ends of two cracks are marked with arrows. **(E)** Microphotograph of the inclusion KK200-9. **(F)** Raman map of the host diamond, showing a halo of enhanced pressure around the HP inclusion (same area as in E; view along [331]). **(G)** Phase-contrast image generated through Raman mapping of Ca-silicates (mapped area corresponds to the central part of E). Areas of laterally high intensity of the bands at ~ 860 cm^{-1} (Ca_2SiO_4; blue), ~ 1050 cm^{-1} ($CaSiO_3$; green) and ~ 356 cm^{-1} ($CaSi_2O_5$; red) are shown (compare Fig. 2). **(H)** Raman map of the diamond PAG02 around the graphite inclusion (view along [110]). For more clarity, the inclusion is overlaid black. The diamond reveals a weak pattern that is reminiscent to growth zoning. **(I)** Graphite inclusion in the diamond PAG07 (view along [111]), microphotograph. **(J)** Raman map of the graphite inclusion. The main crystal is well ordered. Strongly disordered carbon occurs in the surrounding small circular crack. **(K)** Raman map of PAG07 after tilting the sample by 90° (view along [1$\bar{1}$0]). The complex pattern of compression (marked c) and dilation (marked d) in the diamond, caused by extensive volume expansion of the graphite along [001] and accompanying fracturing of the diamond in its (111) plane, is explained by the adjacent sketch.

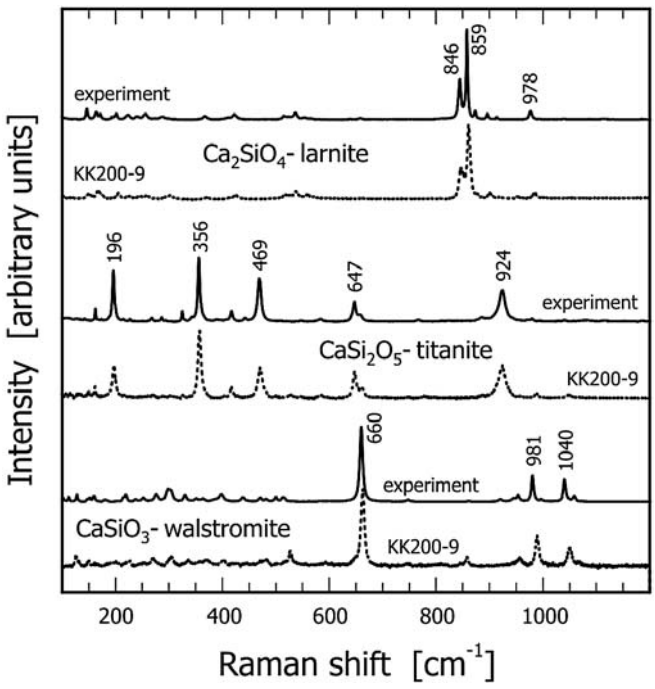

Fig. 2. Raman spectra of three different Ca-silicates in the inclusion KK200-9 (dotted), compared with reference spectra of the same phases (solid) obtained from an experimental product of Gasparik *et al.* (1994). Slightly higher Raman shifts observed from the silicates included in diamond indicate lattice compression due to residual pressure.

inclusion couples (Fig. 1C, E, I), but it was partially preserved, as indicated by noticeable Raman shifts in the spectra of the included minerals. For instance, the main Raman band of coesite ($\tilde{\nu}$ ~ 520.6 cm^{-1} at ambient pressure) was observed at 527.2 cm^{-1}, which indicates a residual pressure of 2.3 ± 0.2 GPa for the inclusion KK200-8 (*cf.* Hemley, 1987).

Residual pressure and strain can also be estimated from the LO = TO mode of the host diamonds (due to the high lattice symmetry, longitudinal and transversal optical lattice vibrations are degenerated and have the same frequency). According to Grimsditch *et al.* (1978), the LO = TO mode ($\tilde{\nu}$ ~ 1332 cm^{-1} at ambient pressure) is shifted between + 0.7/GPa (strain along [111]) and + 2.2 cm^{-1}/GPa (strain along [001]). Consequently, a $\tilde{\nu}$-shift of + 1.8 cm^{-1} observed from diamond PAG07 next to the (001) face of graphite (the expansion of which has caused stress in the diamond along [111]; Fig. 1K) indicates a remnant pressure of ~ 2.6 GPa. This value is in reasonable agreement with an estimate of 2.4 GPa based on unit-cell parameters of the very same graphite inclusion (Glinnemann *et al.*, 2003).

Finally, Raman mapping along 2D planes inside the diamonds showed that areas around HP inclusions in which the diamond is affected by residual pressure and strain show complex patterns (Fig. 1). These haloes may extend to > 300 µm away from inclusions (*e.g.*, Fig. 1K). Non-fractured sectors have always stored higher pressures whereas fractured areas indicate more extensive pressure release (compare Fig. 1C and D). Areas close to the ends of large cracks are in some cases affected by dilative strain that is strong enough to cause apparent "negative pressures" (red coloured areas in Fig. 1D, K).

Our preliminary results indicate that $\tilde{\nu}$ (LO = TO) in diamond is most useful to study its pressure distribution patterns whereas the FWHM of this mode appears more sensitive to strain phenomena. For example, an FWHM-based map of KK200 around the inclusion #8 (Fig. 1B) yielded a strain pattern with a three-fold symmetry that was not observed in the analogous $\tilde{\nu}$-based map. Similarly, the zoning in PAG02 (Fig. 1H) was not revealed by the corresponding $\tilde{\nu}$-based map. Future Raman studies may contribute to a better understanding of the pressure-strain relationships around HP inclusions in diamond.

Acknowledgements: Diamond specimens were kindly made available by De Beers Consolidated Mines Ltd. We are indebted to M. Ziemann and W. Joswig for helpful comments. This work was supported by the Materials Science Research Centre, Mainz. J. G. acknowledges funding from the German Science Foundation (DFG) through grant Wi 1232/18-1. Constructive reviews by R. Kaindl, B. Wopenka and an anonymous expert are gratefully acknowledged.

References

Boppart, H., van Straaten, J., Silvera, I.F. (1985): Raman spectra of diamond at high pressures. *Phys. Rev. B*, **32**, 1423-1425.

Gasparik, T., Wolf, K., Smith, C.M. (1994): Experimental determination of phase relations in the $CaSiO_3$ system from 8 to 15 GPa. *Am. Mineral*., **79**, 1219-1222.

Gillet, P., Sautter, V., Harris, J., Reynard, B., Harte, B., Kunz, M. (2002): Raman spectroscopic study of garnet inclusions in diamonds from the mantle transition zone. *Am. Mineral.*, **87**, 312-317.

Glinnemann, J., Kusaka, K., Harris, J.W. (2003): Oriented graphite single-crystal inclusions in diamond. *Z. Kristallogr.* (in press).

Grimsditch, M.H., Anastassakis, E., Cardona, M. (1978): Effect of uniaxial stress on the zone-center optical phonon of diamond. *Phys. Rev. B*, **18**, 901-904.

Hanfland, M., Syassen, K., Fahy, S., Louie, S.G., Cohen, M.L. (1985): Pressure dependence of the first-order Raman mode in diamond. *Phys. Rev. B*, **31**, 6896-6899.

Hemley, R.J. (1987): Pressure dependence of Raman spectra of SiO_2 polymorphs: α-quartz, coesite and stishovite. *In* Manghnani, M.H. & Syono, Y. (eds.): High-pressure research in mineral physics. Am. Geophys. Union, Washington D.C., 347-359.

Izraeli, E.S., Harris, J.W., Navon, O. (1999): Raman barometry of diamond formation. *Earth Planet. Sci. Lett.*, **173**, 351-360.

Joswig, W., Stachel, T., Harris, J.W., Baur, W.H., Brey, G.P. (1999): New Ca-silicate inclusions in diamonds - tracers from the lower mantle. *Earth Planet. Sci. Lett.*, **173**, 1-6.

Reynard, B., Remy, C., Takir, F. (1997): High-pressure Raman spectroscopic study of Mn_2GeO_4, Ca_2GeO_4, Ca_2SiO_4, and $CaMgGeO_4$ olivines. *Phys. Chem. Minerals*, **24**, 77-84.

Rosenfeld, J.L. & Chase, A.B. (1961): Pressure and temperature of crystallization from elastic effects around solid inclusions in minerals? *Am. J. Sci.*, **259**, 519-541.

Sobolev, N.V., Fursenko, B.A., Goryainov, S.V., Shu, J.F., Hemley, R.J., Mao, H.K., Boyd, F.R. (2000): Fossilized high pressure from the Earth's deep interior: The coesite-in-diamond barometer. *Proc. Natl. Acad. Sci. USA*, **97**, 11875-11879.

Ye, K., Liou, J.-B., Cong, B., Maruyama, S. (2001): Overpressures induced by coesite-quartz transition in zircon. *Am. Mineral.*, **86**, 1151-1155.

Zhao, Y.X. & Spain, I.L. (1989): X-ray diffraction data for graphite to 20 GPa. *Phys. Rev. B*, **40**, 993-997.

Received 2 July 2003
Modified version received 20 August 2003
Accepted 15 September 2003